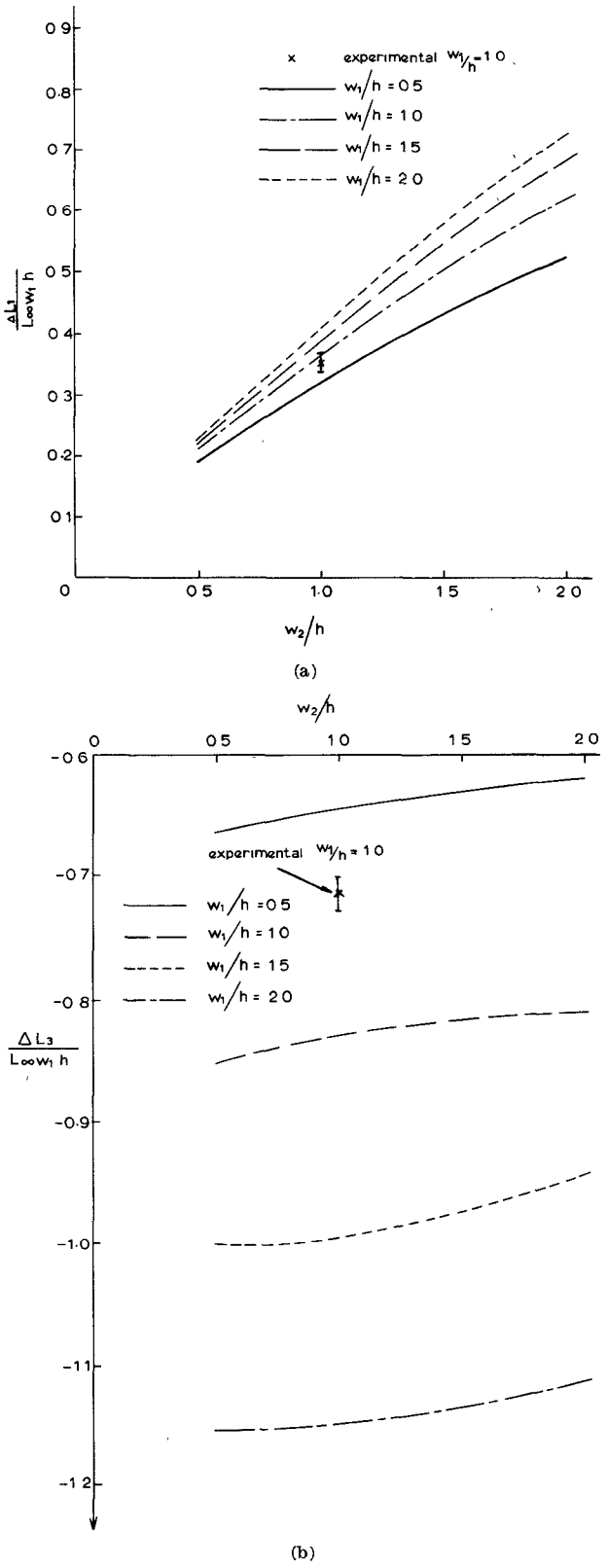

Fig. 6. (a) Calculated value of ΔL_1 normalized to $L_{\infty w1}h$ of the cross junction for different w_1/h and w_2/h. This same set of curves is to be used for estimating normalized ΔL_2. (b) Calculated value of ΔL_3 normalized to $L_{\infty w1}h$ of the cross junction.

Fig. 5(a) with reference planes at QQ', PP', QP, and $Q'P'$. As in the step, the excess current is assumed to be zero outside the area enclosed by the secondary references plane M_1M_1', M_2M_2', N_1N_1', and N_2N_2'. The distance from M_1M_1' to QQ' (and similar distances) was chosen so that the discontinuity inductance was not affected by any increase in this length. The results are summarized in Fig. 6(a) and (b) for different straight-arm ratios. Fig. 6(a) may also be used to evaluate the second inductance by turning the cross by 90°. Only one experimental point due to Easter [4] is available, and comparison with this theory shows that agreement is good for ΔL_1 and ΔL_2, but not for ΔL_3. Again, the disagreement in ΔL_3 is of the same order as our earlier results [1] for the T junction. The straight-through results of step change in width, straight arms of the T, and now the straight arms of the cross give very good agreement with experimental results. The theoretical results when the current goes around corners give poorer agreement with experiment. We may only conclude that the trial functions do not describe the current distribution adequately in these cases.

ACKNOWLEDGMENT

The authors wish to thank B. Easter for help and advice during this work.

REFERENCES

[1] A. F. Thomson and A. Gopinath, "Calculation of microstrip discontinuity inductances," *IEEE Trans. Microwave Theory Tech.*, vol. MTT-23, pp. 648–655, Aug. 1975.
[2] P. Silvester and P. Benedek, "Microstrip discontinuity capacitances for right-angle bends, T junctions, and crossings," *IEEE Trans. Microwave Theory Tech.*, vol. MTT-21, pp. 341–346, May 1973.
[3] A. Farrar and A. T. Adams, "Matrix methods for microstrip three-dimensional problems," *IEEE Trans. Microwave Theory Tech.*, vol. MTT-20, pp. 497–504, Aug. 1972.
[4] B. Easter, "Equivalent circuits of some microstrip discontinuities," *IEEE Trans. Microwave Theory Tech.*, vol. MTT-23, pp. 655–660, Aug. 1975.

A New Integrated Waveguide–Microstrip Transition

J. H. C. VAN HEUVEN, MEMBER, IEEE

***Abstract*—A new waveguide–microstrip transition is described. This design provides wide-band performance (18–26 GHz) and very good reproducibility without the need for variable elements. The circuit is fully integrated on the substrate and the characteristics are much less sensitive to small variations in the dimensions than other known transitions. A narrow-band version has been made for the telecommunication band in particular (17.7–19.7 GHz) with a VSWR less than 1.1 and an attenuation less than 0.25 dB.**

The design can easily be scaled to other frequencies and is especially useful at frequencies above 10 GHz.

INTRODUCTION

The introduction of MIC's in systems created the need for transitions between the conventional transmission lines and microstrip. At lower frequencies (below 10 GHz) a miniature coaxial connector is frequently used for this purpose.

The main problems are to establish a reliable contact between the inner conductor of the connector and the microstrip and to achieve adequate sealing of the circuit. Above 10 GHz such a transition is not satisfactory for most applications. Since many systems at these frequencies require waveguide components (e.g., low-loss filters, antenna horns) a direct waveguide–microstrip transition would be preferable and could solve the contact and sealing prob-

Manuscript received May 29, 1975; revised August 26, 1975.
The author is with the Philips Research Laboratories, Eindhoven, The Netherlands.

lems as well. Such a transition should satisfy the following conditions: low reflection, low attenuation, wide band, and reproducible performance. The reproducibility is of particular importance to accurate measurements of circuits and devices in microstrip with the use of standard waveguide equipment.

Several different waveguide–microstrip transitions have been described in the literature. Small and simple structures are obtained with antenna-type transitions, integrated on the substrate, the equivalent of the waveguide–coaxial line transition [1], [2]. A disadvantage of these designs is the small bandwidth so far obtained and the sensitivity of the performance to small variations in the dimensions. A wide-band transition can be achieved with a stepped ridge waveguide transformer [2]–[4]. The construction, however, is more complicated than that of the precious one and the results also depend critically on the dimensions. A new wide-band integrated waveguide–microstrip transition is described in the following, which overcomes these difficulties to a large extent.

NEW DESIGN

The basic idea is the use of gradually tapered ridges at opposite sides of a dielectric substrate, concentrating and rotating the electrical field into a parallel line. This symmetrical line is matched by a balancing transformer (balun) to the asymmetrical microstrip. An outline of the substrate inserted in the waveguide is given in Fig. 1. The position of the circuit pattern in the guide is indicated in the cross section along the z axis in Fig. 2.

The following parts can be distinguished in Fig. 2: 1) the tapered ridges a on the front and the back of the substrate; 2) the symmetrical line section b; 3) the balun section c; 4) the microstrip d.

The ridges and the ground plane of the microstrip are connected to the wall of the guide along the lines l. The balun section is obtained by slots in the ground plane and a reduction of the upper strip width in order to maintain a constant characteristic impedance (50 Ω). Fig. 3 shows an exploded view of the enclosure. Two transitions have been cascaded in such a way that a symmetrical waveguide–microstrip–waveguide section has been obtained. This construction facilitates the measurements, carried out with waveguide components and affords the use of a matched load in waveguide. The serrated chokes avoid the need for electrical contact with the enclosure [5]. Propagation through the waveguide, except along the microstrip, is prevented by the ground plane dividing the guide into two parallel guides with a cutoff frequency far above the waveguide band. The form of the tapers and the length of the slots and the serrated chokes has been experimentally optimized. The reproducibility is very good, because all critical dimensions are exactly reproduced by photolithography. The position of the substrate in the guide is not critical. The height of the guide is increased to compensate for the loading of the guide by the silica substrate. The higher the dielectric constant and the thicker the substrate, the more the height of the guide should be increased. A relatively low dielectric constant is consequently preferred in order to minimize the necessary compensation.

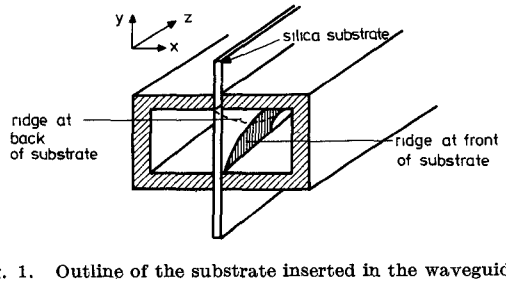

Fig. 1. Outline of the substrate inserted in the waveguide.

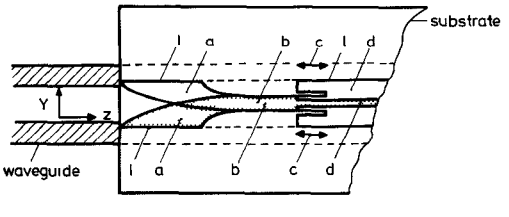

Fig. 2. Position of the planar circuit in the waveguide. See text for the nomenclature.

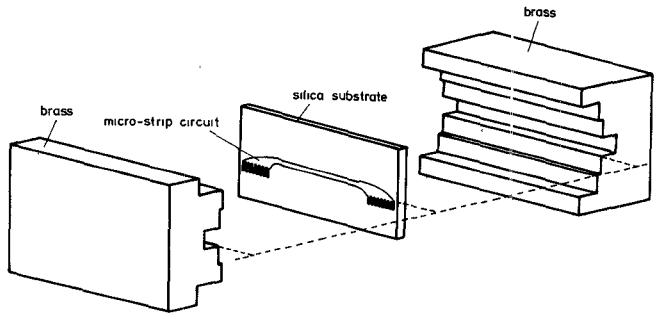

Fig. 3. Exploded view of two cascaded transitions (waveguide–microstrip–waveguide).

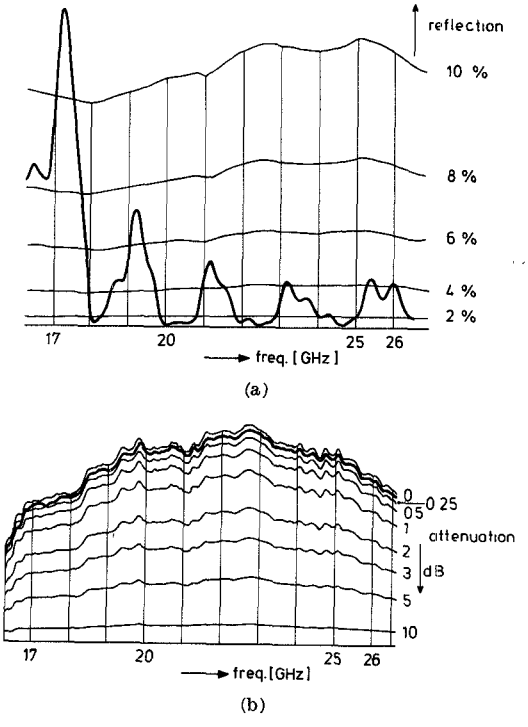

Fig. 4. Curves of the waveguide mount of Fig. 3 with a silica substrate. (a) Reflection curve. (b) Transmission curve.

The circuit described in this short paper uses a silica substrate (2.5 × 5 cm²) with a thickness of 0.5 mm (dielectric constant 3.8). The reflection of the waveguide mount containing a silica slab only, terminated at one side by a matched load in standard waveguide, is depicted in Fig. 4(a) in the frequency band from 17 to 26 GHz. The curve represents the reflection coefficient of the structure depicted in Fig. 3. Maxima and minima in the response are caused by interference. The length of the section is 5 cm. The reflection of *one* transition (substrate without metallization) is thus half of the measured value (negligible losses): max 5 percent (VSWR 1.11) from 18–26 GHz in Fig. 4(a). This figure can be further improved if required. The loss of the section is presented in Fig. 4(b) and proves to be about 0.2 dB over the waveguide band. Fig. 5 shows the actual circuit.

The following dimensions have been used (approximate values):

length of slot c (Fig. 2) ~4.0 mm;

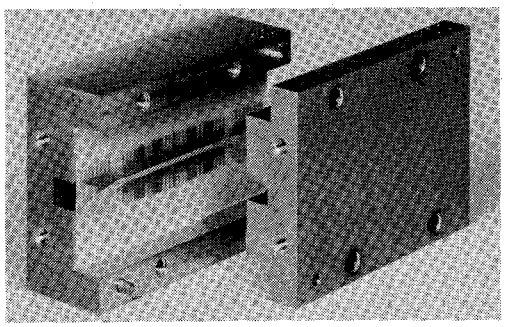

Fig. 5. Actual planar circuit in waveguide mount.

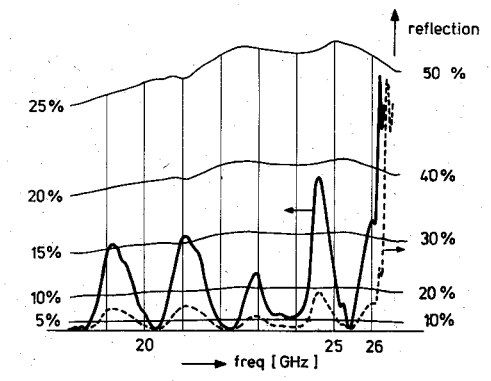

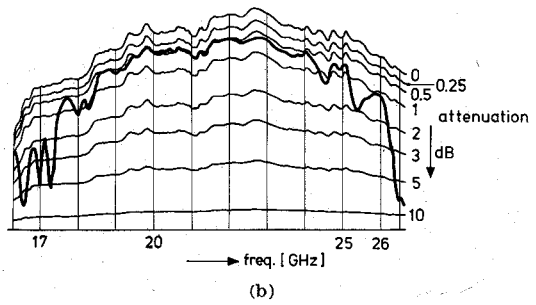

Fig. 6. Curves of two cascaded wide-band transitions. (a) Reflection curve. (b) Transmission curve.

width of slot c (Fig. 2)	~0.5 mm;
length of l (Fig. 2)	~7.5 mm;
width of strip b (Fig. 2)	~1.5 mm;
width of strip d (Fig. 2)	~1.0 mm;
length of serrated chokes (Fig. 5)	~1.7–2.5 mm.

A wide-band 18–26 GHz transition (Type A) and a narrow-band 17.5–23 GHz (Type B) have been designed, the latter in particular for the telecommunication bands. The two circuits have different lengths of the slots (section c in Fig. 2) and of the serrated chokes. The performance of one transition can be approximated by dividing the reflection and the attenuation of the symmetrical structure by two. The attenuation includes losses in the microstrip line length (about 2 cm). The measured curves are displayed in Figs. 6 and 7 for both Types A and B, respectively, and are tabulated in the following for *one* transition.

	Reflection (percent)	VSWR	Attenuation (dB)	Band (GHz)
A	10	1.22	1.0	18–26
	10	1.22	0.5	18–25
	7	1.15	0.5	18–24
B	5	1.10	0.5	17.5–23
	5	1.10	0.25	17.7–19.7

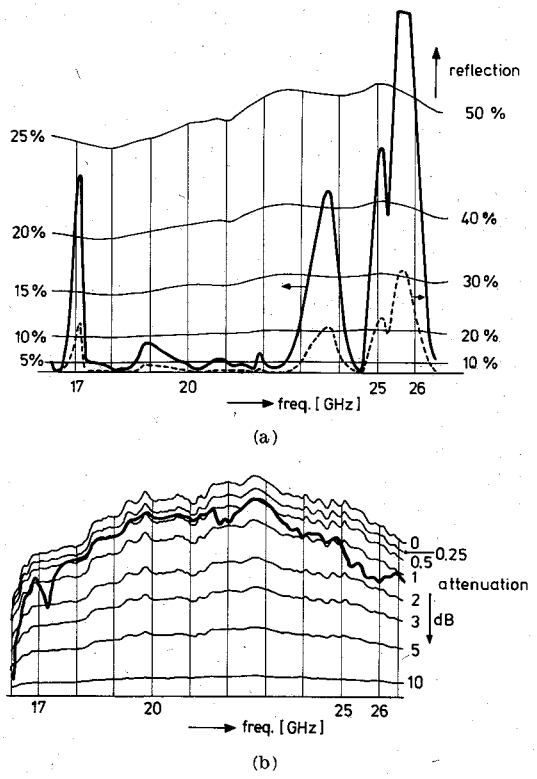

Fig. 7. Curves of two cascaded transitions, optimized for the band 17.7–19.7 GHz. (a) Reflection curve. (b) Transmission curve.

Further optimization is possible by applying a stepped impedance balun section at the cost of an increased length of the transition and by suppressing low-Q resonances in the enclosure. These resonances are excited by the serrated chokes in the longitudinal slots in the waveguide. Some absorbing material in the slot is sufficient to suppress the resonance, slightly affecting the transmission loss and the reproducibility. The same results have been obtained with three different circuits in two different waveguide mounts, proving that this design is not critical to small changes in the dimensions of the mount and in the position of the substrate in the waveguide. The critical parts are located on the substrate. Scaling to other frequency bands is not difficult, by changing all the dimensions (except the strip widths) according to the wavelength and to the appropriate waveguide. In practical cases only one transition will be used between the waveguide and the microstrip circuit. The waveguide may be short-circuited at the ground plane side of microstrip at some arbitrary distance from the balun section (in our case at least 10 mm). At the strip side of the substrate the waveguide height can be increased up to the required width of the enclosure of the microstrip circuit. This dimension should be kept small in order to keep the cutoff frequency of the enclosure below the operating frequency, if possible.

ACKNOWLEDGMENT

The author wishes to thank F. C. de Ronde for suggestions and discussions resulting in this design, J. Timmers for carrying out the measurements, and A. G. van Nie for supplying the circuits.

REFERENCES

[1] B. Glance and R. Trumbarulo, "A waveguide to suspended stripline transition," *IEEE Trans. Microwave Theory Tech.* (Lett.), vol. MTT-21, pp. 117–118, Feb. 1973.

[2] E. A. Oxley, "Hybrid microwave integrated circuits for mm wavelength," in *Dig. 1972 IEEE-GMTT Int. Microwave Symp.*, pp. 224–226.

[3] E. A. Schneider, "Microwave and mm wave hybrid integrated circuits for radio systems," *Bell Syst. Tech. J.*, vol. 48, pp. 1703–1725, July–Aug. 1969.

[4] T. Araki and M. Hirayama, "A 20-GHz integrated balanced mixer," *IEEE Trans. Microwave Theory Tech. (Special Issue on Microwave Integrated Circuits)*, vol. MTT-19, pp. 638–643, July 1971.
[5] K. Tomiyasu and J. J. Bolus, "Characteristics of a new serrated choke," *IRE Trans. Microwave Theory Tech.*, vol. MTT-4, pp. 33–36, Jan. 1956.

Oscillation Characteristics of Millimeter-Wave IMPATT Diodes Mounted in Low-Impedance Waveguide Mounts

M. AKAIKE, H. KATO, AND S. YUKI

***Abstract*—Experiments on dc-bias-current-tuned IMPATT diodes mounted in low-impedance waveguide mounts are described. Broad-band bias-current-tuned IMPATT oscillators were obtained which cover almost the full waveguide band; 20-, 24-, and 18-GHz tuning bandwidths were obtained with the R-500, R-620, and R-740 waveguide, respectively. From experiments it became evident that there are some suitable relations for broad-band bias tuning among the diode breakdown voltage, the oscillation frequency, and the waveguide dimension. The results are very useful for the design of the circuit and diode parameter for broad-band millimeter-wave IMPATT sweep oscillators. The feasibility of applying bias-current-tuned IMPATT oscillators to a broad-band measuring instrument is expected.**

I. INTRODUCTION

Many workers have attempted to enlarge the tunable bandwidth of millimeter-wave IMPATT oscillators [1]–[5] in order to apply IMPATT oscillators to the local oscillators in a millimeter-wave transmission system or in order to construct measuring instruments in the millimeter-wave range.

Three schemes for tuning an IMPATT oscillator are possible: 1) mechanical tuning by varying the position of a movable short; 2) tuning by varying the dc bias current of an IMPATT diode; and 3) tuning by varying the reactance or susceptance of the external circuit electrically, for example, by varying the dc bias voltage of a varactor diode located near the IMPATT diode.

The authors previously reported a mechanically tunable IMPATT oscillator in the 50-GHz range, where a 14-GHz tuning bandwidth was obtained by varying the position of a movable waveguide short [2].

The purpose of this paper is to present experimental results on the oscillation characteristics of dc bias-current-tuned IMPATT diodes mounted in low-impedance waveguide mounts (characteristic impedance is about 70 Ω).

The phenomena which have been found in the course of experiments are very useful in designing broad-band IMPATT sweep oscillators.

In Section II, diodes, frequency ranges, and waveguides which were used in the experiments are summarized. The circuit construction of the IMPATT oscillators is described in Section III. In Section IV, the experimental results are presented. The experimental results contain 1) the relation with respect to oscillation frequency, diode breakdown voltage, and the width of the rectangular waveguide in which the IMPATT diode is mounted; 2) oscillation characteristics obtained with various waveguide sizes; and 3) comparison with a mechanically tunable mode of oscillation.

Manuscript received March 11, 1974; revised August 26, 1975.

The authors are with the Electrical Communication Laboratory, Nippon Telegraph and Telephone Public Corporation, Yokosuka-shi, Kanagawa-ken 238-03, Japan.

II. DIODES AND FREQUENCY RANGE

Experiments covered a frequency range of 19–92 GHz with 5 kinds of waveguides (R-220, R-320, R-500, R-620, and R-740), and diodes with 8 different breakdown voltages (V_B = 9.8–38 V). They are listed in Fig. 1 and Table I.

The diodes are of the silicon single-drift-region type. The diode with V_B = 38 V is encapsulated and other diodes are unencapsulated. Fig. 2 shows the structure of an unencapsulated diode.

Diodes with breakdown voltages of 9.8–21 V were fabricated in the Musashino Electrical Communication Laboratory, NTT. Typical oscillation power of a diode with V_B = 13.8 V is about 23 dBm at 80 GHz [6]. In experiments on bias-current-tuned oscillators, this diode was used in the 60-GHz range with an R-620 waveguide. The diode with V_B = 38 V is commercially available as V749 (manufactured by the Nippon Electric Co.) and typical oscillation power is more than 23 dBm at 20 GHz [7].

III. OSCILLATOR MOUNT STRUCTURE

Fig. 3 shows a cross-sectional view of the IMPATT oscillator. The oscillator consists of five parts: an IMPATT diode which is mounted on a copper heat sink, a coaxial line, a rectangular waveguide of

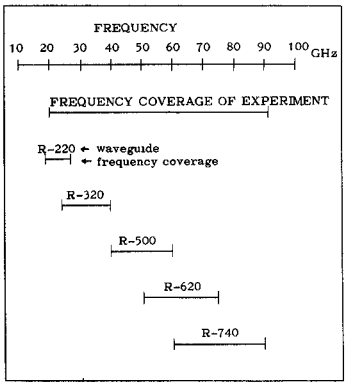

Fig. 1. Waveguide and its frequency coverage. (R-: standardized by the International Electrotechnical Commission.)

TABLE I
DIODE BREAKDOWN VOLTAGE

DIODE #	BREAKDOWN VOLTAGE	Maximum oscillation power NOTE ( ) and its frequency
# 1	9.8 V	
# 2	10.1 V	
# 3	11.2 V	
# 4	13.8 V	* 82 GHz, 23.3 dBm
# 5	17.2 V	** 42 GHz, 24.1 dBm
# 6	18.6 V	** 40 GHz, 19.7 dBm
# 7	21 V	** 39 GHz, 20.8 dBm
# 8	38 V	*** 20 GHz, 23 dBm

* [6].
** Private letter from Dr. K. Suzuki and Dr. M. Ohmori.
*** [7].

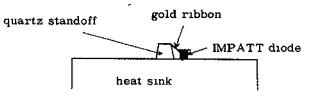

Fig. 2. Structure of an unencapsulated IMPATT diode.